



## NRC Publications Archive Archives des publications du CNRC

### **Magnetic properties of the $S=3/2$ geometrically frustrated double perovskites $\text{La}_2\text{LiRuO}_6$ and $\text{Ba}_2\text{YRuO}_6$**

Aharen, Tomoko; Greedan, John E.; Ning, Fanlong; Imai, Takashi; Michaelis, Vladimir; Kroeker, Scott; Zhou, Haidong; Wiebe, Chris R.; Cranswick, Lachlan M. D.

This publication could be one of several versions: author's original, accepted manuscript or the publisher's version. / La version de cette publication peut être l'une des suivantes : la version prépublication de l'auteur, la version acceptée du manuscrit ou la version de l'éditeur.

For the publisher's version, please access the DOI link below. / Pour consulter la version de l'éditeur, utilisez le lien DOI ci-dessous.

#### **Publisher's version / Version de l'éditeur:**

<https://doi.org/10.1103/PhysRevB.80.134423>

*Physical Review B*, 80, 13, 2009-10-28

#### **NRC Publications Record / Notice d'Archives des publications de CNRC:**

<https://nrc-publications.canada.ca/eng/view/object/?id=4adb93d4-bb91-436a-85a7-cf2eaaf9720e>

<https://publications-cnrc.canada.ca/fra/voir/objet/?id=4adb93d4-bb91-436a-85a7-cf2eaaf9720e>

Access and use of this website and the material on it are subject to the Terms and Conditions set forth at

<https://nrc-publications.canada.ca/eng/copyright>

READ THESE TERMS AND CONDITIONS CAREFULLY BEFORE USING THIS WEBSITE.

L'accès à ce site Web et l'utilisation de son contenu sont assujettis aux conditions présentées dans le site

<https://publications-cnrc.canada.ca/fra/droits>

LISEZ CES CONDITIONS ATTENTIVEMENT AVANT D'UTILISER CE SITE WEB.

**Questions?** Contact the NRC Publications Archive team at

PublicationsArchive-ArchivesPublications@nrc-cnrc.gc.ca. If you wish to email the authors directly, please see the first page of the publication for their contact information.

**Vous avez des questions?** Nous pouvons vous aider. Pour communiquer directement avec un auteur, consultez la première page de la revue dans laquelle son article a été publié afin de trouver ses coordonnées. Si vous n'arrivez pas à les repérer, communiquez avec nous à PublicationsArchive-ArchivesPublications@nrc-cnrc.gc.ca.



# Magnetic properties of the $S = \frac{3}{2}$ geometrically frustrated double perovskites $\text{La}_2\text{LiRuO}_6$ and $\text{Ba}_2\text{YRuO}_6$

Tomoko Aharen,<sup>1</sup> John E. Greedan,<sup>1,2</sup> Fanlong Ning,<sup>2,3</sup> Takashi Imai,<sup>2,3,4</sup> Vladimir Michaelis,<sup>5</sup> Scott Kroeker,<sup>5</sup> Haidong Zhou,<sup>6</sup> Chris R. Wiebe,<sup>6,7</sup> and Lachlan M. D. Cranswick<sup>8</sup>

<sup>1</sup>Department of Chemistry, McMaster University, Hamilton, Ontario, Canada L8S 4M1

<sup>2</sup>Brockhouse Institute for Materials Research, McMaster University, Hamilton, Ontario, Canada L8S 4M1

<sup>3</sup>Department of Physics and Astronomy, McMaster University, Hamilton, Ontario, Canada L8S 4M1

<sup>4</sup>Canadian Institute for Advanced Research, Toronto, Ontario, Canada M5G 1Z8

<sup>5</sup>Department of Chemistry, University of Manitoba, Winnipeg, Manitoba, Canada R3T 2N2

<sup>6</sup>Department of Physics, Florida State University, Tallahassee, Florida 32310-4005, USA

<sup>7</sup>National High Magnetic Field Laboratory, Florida State University, Tallahassee, Florida 32310-4005, USA

<sup>8</sup>Canadian Neutron Beam Centre, National Research Council, Chalk River Laboratories, Chalk River, Ontario, Canada K0J 1J0

(Received 7 August 2009; revised manuscript received 29 September 2009; published 28 October 2009)

Two  $B$ -site ordered double perovskites,  $\text{Ba}_2\text{YRuO}_6$  and  $\text{La}_2\text{LiRuO}_6$ , have been reinvestigated as part of a systematic study of geometric magnetic frustration in this class of oxide materials. Both involve  $\text{Ru}^{5+}(4d^3, S = 3/2)$  as the magnetic ion residing on a face-centered-cubic lattice—one of the canonical frustrated lattices. Results from dc susceptibility, neutron-diffraction, heat-capacity,  $^7\text{Li}$  and  $^{89}\text{Y}$  NMR studies are presented.  $\text{La}_2\text{LiRuO}_6$  ( $P2_1/n$ ) shows long-range antiferromagnetic order below 24 K from  $^7\text{Li}$  NMR, heat-capacity and magnetic-susceptibility (Fisher's heat-capacity) data which is well below the susceptibility maximum at 30 K. Analysis of the entropy loss and the  $^7\text{Li}$  data indicates the importance of short-range spin correlations at higher temperatures, consistent with a frustrated system.  $\text{Ba}_2\text{YRuO}_6$  retains  $Fm\bar{3}m$  symmetry found at room temperature down to 2.8 K with cell constants,  $a = 8.33559(9)$  and  $a = 8.3239(5)$  Å, respectively. However,  $^{89}\text{Y}$  magic-angle-spinning NMR detects a very low  $\sim 1\%$  site mixing between Y and Ru ions. Magnetic-susceptibility data are more complex than reported previously with two broad peaks around 37 and 47 K. The transition temperature is 36 K from heat capacity and variable-temperature neutron-diffraction data. The Weiss temperatures and frustration indices,  $|\theta|/T_N$ , for  $\text{Ba}_2\text{YRuO}_6$  are  $-522$  K and 16 while much smaller values are observed for  $\text{La}_2\text{LiRuO}_6$ ,  $-184$  K and 8, which can be attributed to the monoclinic structural distortion in the latter which weakens the superexchange interactions.

DOI: [10.1103/PhysRevB.80.134423](https://doi.org/10.1103/PhysRevB.80.134423)

PACS number(s): 75.50.Lk, 75.50.Ee, 76.60.-k, 61.05.F-

## I. INTRODUCTION

Geometrically frustrated antiferromagnetic (AF) materials have attracted considerable interest over the past few years.<sup>1</sup> Such compounds often exhibit rather exotic magnetic ground states such as the spin glass, spin liquid, or spin ice states instead of long-range order as might be expected from the third law of thermodynamics. Among such materials, the  $B$ -site ordered double perovskites,  $A_2BB'O_6$ , are a relatively less studied class. In this case a magnetic ion resides on the  $B'$  site while  $B$  is nonmagnetic. Both the  $B$  and  $B'$  sites constitute interpenetrating face-centered-cubic sublattices, Fig. 1, which, if the exchange constraint between nearest  $B'$  neighbors is antiferromagnetic, the basic criteria for geometric frustration are satisfied. The conditions for  $B$ - $B'$  site ordering have been presented in the form of a phase diagram<sup>2</sup> and the space-group family tree has been constructed.<sup>3</sup> For tolerance factors near unity, cubic symmetry is usually found which in this case is  $Fm\bar{3}m$ . As the tolerance factor decreases the symmetry lowers and one finds cases of  $I4/m$ ,  $P2_1/n$ , or  $P-1$ , for example.

A notable feature of  $B$ -site ordered double perovskites is the versatility of this structure type to chemical substitution. Indeed, much of the periodic table can be accommodated.<sup>2</sup> The large  $A$ -site ions are generally from group 2 or 3 and the  $B$  and  $B'$  ions from the transition series  $3d-5d$  and  $4f$  or

small group 1–3 ions. Thus, this class of perovskites permits the systematic study of the effects of changes in, for example, the spin quantum number,  $S$ , and the space-group and  $B'$  point-group symmetries, which controls the “orbital ordering,” on magnetic properties. For example, in the  $Fm\bar{3}m$  structure the site symmetry at  $B'$  is rigorously cubic,  $m\bar{3}m$ , while for  $P2_1/n$  this symmetry is reduced to  $-1$ . Thus, for electronic configurations of the type  $t_{2g}^n$ , the  $t_{2g}$  orbitals remain degenerate in  $m\bar{3}m$  but this degeneracy will be lifted in  $-1$ . In this work the  $B$  site contains diamagnetic  $\text{Y}^{3+}$  and the  $B'$  site is occupied by  $\text{Ru}^{5+}$ ,  $4d^3(t_{2g}^3)$  and  $S = \frac{3}{2}$ . Note that this ion is always an orbital singlet in a crystal field of octahedral symmetry, neglecting spin-orbit coupling, and orbital ordering will not be an issue. In subsequent papers, studies of materials with controlled space group and local symmetry but with quantum spins,  $S=1$  and  $S=\frac{1}{2}$  will be presented. There exists already evidence that quantum spin double perovskites behave rather differently than the  $S=\frac{3}{2}$  analogs. For example the  $S=\frac{1}{2}$  compounds  $\text{Sr}_2\text{CaReO}_6$  ( $P2_1/n$ ) (Ref. 4) and  $\text{Sr}_2\text{MgReO}_6$  ( $I4/m$ ) (Ref. 5) do not show long-range AF order but instead, spin-glass ground states.

A number of materials with  $Fm\bar{3}m$  symmetry have been studied in the early 1990s such as the series  $\text{Ba}_2BRuO_6$ , where  $B=Y$  and  $\text{Lu}$ .<sup>6</sup> These phases were reported to be well-ordered  $Fm\bar{3}m$  double perovskites which showed AF order (fcc type I) at  $\sim 35$  K for the  $B=\text{Lu}$  compound, the Y case

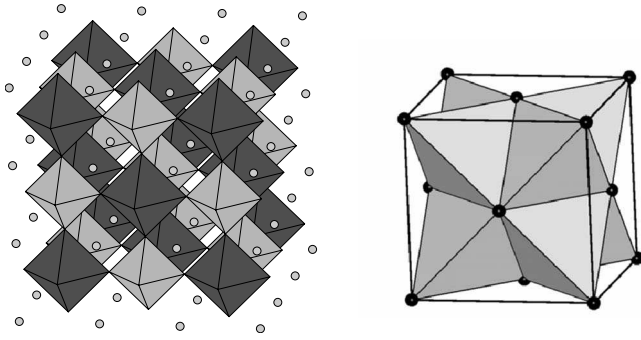


FIG. 1. (Left) The crystal structure of  $B$ -site ordered double perovskite,  $A_2BB'O_6$ . The gray spheres, light gray octahedral, and dark gray octahedra represent  $A$  ions,  $BO_6$  octahedra, and  $B'O_6$  octahedra, respectively. (Right) The geometrically frustrated face-centered-cubic lattice of edge sharing tetrahedra formed by both the  $B$  and  $B'$  sites.

was not reported. As well, large, negative Weiss temperatures in the range of  $-630$  K were found suggesting a high degree of frustration by the frustration index criterion,  $f \sim |\theta|/T_N \sim 18$ .<sup>7</sup>

A  $Ru^{5+}$  based double perovskite with lower symmetry ( $P2_1/n$ ),  $La_2LiRuO_6$ , has been studied more recently.<sup>8</sup> Again, this compound showed long-range AF order (fcc type I) at 4 K and a susceptibility maximum at 30 K.  $^7Li$  magic-angle-spinning (MAS) nuclear magnetic resonance (NMR) indicated only one sharp peak which along with the refinement of neutron-diffraction data indicated a well-ordered double perovskite. The exact value of  $T_N$  was not reported but assuming a value of  $\sim 30$  K and given  $\theta_C = -167$  K,  $La_2LiRuO_6$  is significantly less frustrated,  $f \sim 6$ , than  $Ba_2YRuO_6$ ,  $f \sim 18$ , as already mentioned.

In this work,  $La_2LiRuO_6$  and  $Ba_2YRuO_6$  have been reinvestigated within the context of geometric magnetic frustration. For the former,  $^7Li$  NMR studies along with heat capacity and magnetic-susceptibility data provide an accurate measure of  $T_N$  which is significantly lower than reported previously. For the latter,  $^{89}Y$  MAS NMR indicate some degree of Y/Ru site disorder which is not easily detected from the neutron data. As well, the magnetic susceptibility is more complex than reported previously, showing signs of significant short-range correlations above the critical temperature which is confirmed by neutron diffraction. Heat-capacity measurements determine an accurate value for  $T_N$ , which was not reported in earlier studies. The study of these two materials provides a context for subsequent papers which will describe the results of lowering the spin quantum number to 1 and  $\frac{1}{2}$  in a set of exactly isostructural materials.

## II. EXPERIMENTAL PROCEDURES

$La_2LiRuO_6$  and  $Ba_2YRuO_6$  were prepared using conventional solid-state reactions. For  $La_2LiRuO_6$ ,<sup>7</sup> a stoichiometric mixture of  $La_2O_3$  (Aldrich, 99.9%) (prefired at  $900^\circ C$  to remove surface contaminants),  $RuO_2$  (Alfa Aesar, 99.95%), and 10% excess of  $Li_2CO_3$  (J.T. Baker Chemical Co., 99.1%) was ground, pelletized, heated to  $600^\circ C$ , and kept at that

temperature overnight. This was followed by gradual heating up to  $700^\circ C$  for 1 day and a final firing at  $900^\circ C$  for about 2 days to complete the reaction. For  $Ba_2YRuO_6$ ,<sup>6</sup> a stoichiometric mixture of the starting reagents,  $BaCO_3$  (T. Baker Chemical Co.),  $Y_2O_3$  (Alfa Aesar, 99.9%) (preheated), and  $RuO_2$  (Alfa Aesar, 99.95%) was ground, pelletized, and heated to  $1350^\circ C$  for a total of 5 days with intermittent regrinding. In addition to that nonmagnetic analogs for both samples,  $La_2LiIrO_6$  and  $Ba_2YTaO_6$ , were prepared. For  $La_2LiIrO_6$ , a mixture of  $La_2O_3$  (preheated),  $Li_2CO_3$  (10% excess), and Ir powder (CERAC, 99.9%) was heated in  $O_2$  flow and kept at 1123 K for 96 h. For  $Ba_2YTaO_6$ , a stoichiometric mixture of  $BaCO_3$ ,  $Y_2O_3$ , and  $Ta_2O_5$  (Alfa Aesar 99.99% and SPEX) was heated in air at  $1350^\circ C$  for about 3 days in total with intermediate regrinding. The purity of the samples was tested by x-ray diffraction using a Guinier-Hägg camera with  $Cu K\alpha_1$  radiation.

Magnetic susceptibility was measured for both samples within the temperature range 2 K (or 5 K) to 300 K using a quantum design magnetic properties measurement system superconducting quantum interference device magnetometer at McMaster University. Zero-field-cooling (ZFC) and field-cooling (FC) data were obtained with an applied field of 500 Oe.

Heat-capacity measurements were carried out for  $La_2LiRuO_6$  and  $Ba_2YRuO_6$  using an Oxford Maglab over the temperature ranges of 8–49.9 and 5–56.5 K, respectively. Also, the heat capacity for  $La_2LiRuO_6$  and its lattice match compound were measured at Florida State University using a quantum design physical properties measurement system. system in the temperature range of 2–70 K. To extract magnetic heat capacity, the nonmagnetic analogs of both samples,  $La_2LiIrO_6$  and  $Ba_2YTaO_6$ , were prepared and the heat capacities of both samples were subtracted as lattice contribution on total heat capacities.

Neutron-diffraction data were obtained for  $Ba_2YRuO_6$  on the C2 diffractometer at the Canadian Neutron Beam Centre operated by the National Research Council of Canada at the Chalk River laboratories of Atomic Energy of Canada. The data were collected at 2.8, 20, 30, 33, 35, 40, and 298 K with neutron wavelengths of 2.7319 Å and/or 1.3305 Å depending on measurement temperature. The crystal structure and magnetic structures were refined using GSAS (Ref. 9) and FULLPROF.<sup>10</sup>

For  $La_2LiRuO_6$ , the  $^7Li$  NMR spin-lattice relaxation rate,  $1/T_1$ , as a function of temperature was measured at McMaster University over the temperature range from 23.3 to 290 K. For  $Ba_2YRuO_6$ ,  $^{89}Y$  magic-angle-spinning solid-state nuclear magnetic resonance was carried out in the Department of Chemistry at the University of Manitoba. The spectrum was acquired using a Bloch pulse on a Varian Inova<sup>Unity</sup> 600 (14.1 T) spectrometer operating at a Larmor frequency,  $\nu_L$  of 29.36 MHz. The black powdered sample was packed in a  $ZrO_2$  MAS rotor with a 22  $\mu l$  fill volume and spun to  $20\,000 \pm 6$  Hz. Acquisition was carried out at room temperature using a  $30^\circ$  tip angle (rf of 42 kHz) on a 3.2 mm DR (H/F-X) Chemagnetics MAS probe, 470 784 coadded transients were collected with a recycle delay of 0.5 s. All spectra were referenced with respect to  $2M Y(NO_3)_3$  at 0.0 ppm.

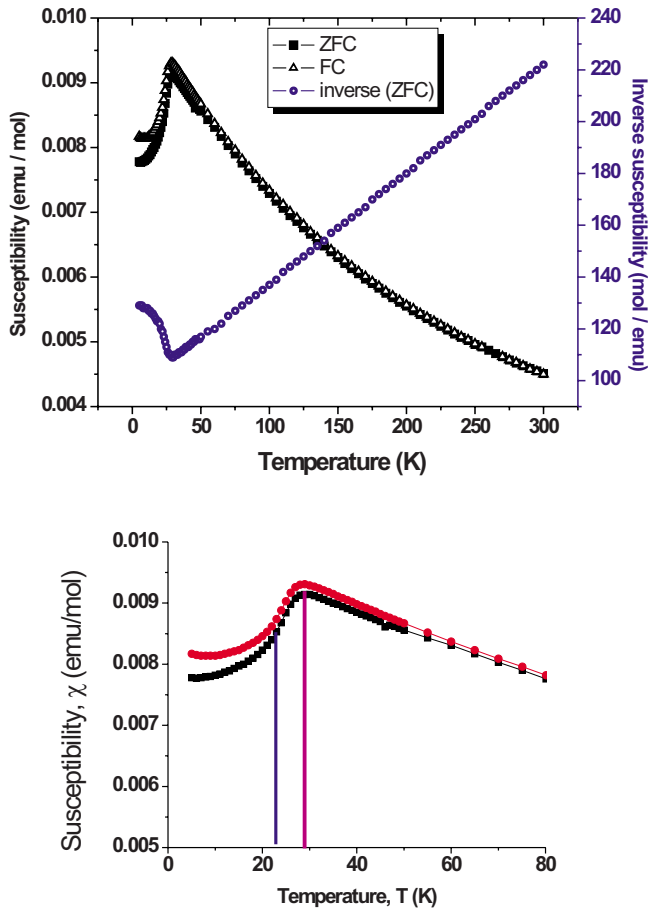


FIG. 2. (Color online) (Top) The temperature dependence of the magnetic susceptibility and inverse magnetic susceptibility of  $\text{La}_2\text{LiRuO}_6$ . FC data were measured with an applied field of 500 Oe. (Bottom) The susceptibility near the temperature region around the transition. The right vertical line marks the susceptibility maximum and the left line locates the transition temperature from the heat capacity and NMR measurements.

### III. RESULTS AND DISCUSSION

#### A. $\text{La}_2\text{LiRuO}_6$

The obtained powder sample was tested by x-ray diffraction and confirmed to be single phase. The temperature dependence of the magnetic susceptibility was measured as shown in Fig. 2. The data were fitted to a Curie-Weiss law with inclusion of a small temperature-independent term,  $\chi = C/(T - \theta) + \chi(\text{TIP})$ , giving the parameters  $C = 1.93(5)$  emu K/mol,  $\theta = -185(5)$  K, and  $\chi(\text{TIP}) = 5.1(5) \times 10^{-4}$  emu/mol. The Curie constant is in reasonable agreement with the expected spin-only value for a  $S = \frac{3}{2}$  ion, 1.87 emu K/mol, and  $\theta$  is slightly larger than that reported in Ref. 8,  $-167$  K. The bottom of Fig. 2 shows the low-temperature data indicating a maximum at 29–30 K, as reported previously, and a ZFC/FC divergence below  $\sim 70$  K. These data were analyzed further by plotting  $d\chi T/dT$  vs  $T$ , i.e., the Fisher heat capacity,<sup>11</sup> shown in Fig. 3, in which the relatively sharp peak at  $\sim 24$  K indicates that this is the true  $T_N$  for this material.

To verify this, the thermal heat capacity of  $\text{La}_2\text{LiRuO}_6$  was measured from 2 to 70 K. Note, Fig. 4, the somewhat

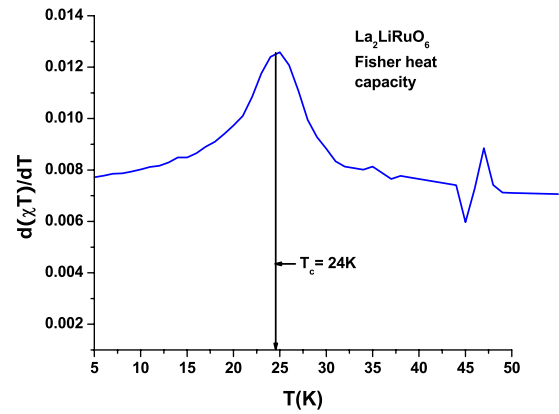


FIG. 3. (Color online) Fisher's heat capacity of  $\text{La}_2\text{LiRuO}_6$  (Ref. 11).

broad maximum at 23–24 K, whereas one might have expected a sharper  $\lambda$ -type anomaly. Shown also are data for the lattice match material,  $\text{La}_2\text{LiIrO}_6$ . In this compound the  $\text{Ir}^{5+}(5d^4)$  ion is a single-ion singlet state and has only a very weak temperature-independent paramagnetic contribution.<sup>12</sup> Subtraction of the lattice match data, shown in the inset, sharpens the peak somewhat. The subtracted magnetic component of heat capacity indicates that about 53.7% of the theoretical total entropy,  $S = R \ln(2S + 1)$ , where  $R$  is the gas constant and  $S$  is the spin quantum number, was lost during this transition. This suggests that short-range correlations at higher temperatures are important which is consistent with a high level of frustration in this material.

Finally, further insight can be provided by study of the temperature dependence of the  $^7\text{Li}$  nuclear-spin-lattice relaxation rate ( $1/T_1$ ), Fig. 5 as the NMR experiment probes the local, low-frequency spin dynamics. Note first that the data are roughly temperature independent above  $\sim 150$  K. This is indicative of paramagnetic (uncorrelated spins) behavior in the exchange narrowing limit as the electron spins fluctuate

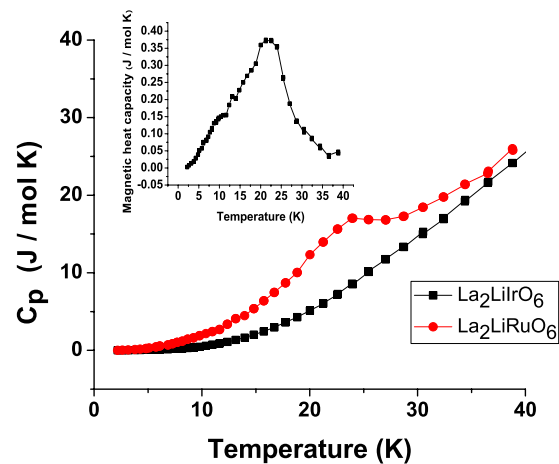


FIG. 4. (Color online) The heat capacity of  $\text{La}_2\text{LiRuO}_6$  and the lattice match compound,  $\text{La}_2\text{LiIrO}_6$ . The magnetic heat capacity shows a somewhat broadened peak centered around 23 K. The inset shows the magnetic heat capacity,  $C_{\text{mag}}/T$  versus  $T$ , from which the magnetic entropy of this compound was calculated. The entropy loss below 40 K is 54% of the theoretical total. (See text).

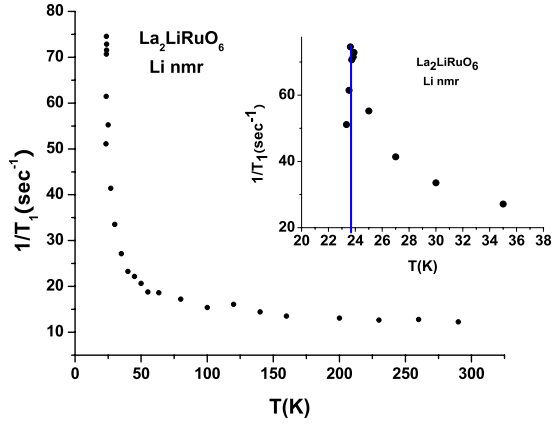


FIG. 5. (Color online) The  ${}^7\text{Li}$  nuclear-spin-lattice relaxation rate,  $1/T_1$ , as a function of temperature. The inset shows the divergence near the transition temperature, 24 K.

rapidly. Below about 70 K, which is also roughly the temperature for which the ZFC/FC divergence in the bulk susceptibility becomes detectable,  $(1/T_1)$  begins to increase, indicating the onset of short-range spin-spin correlations. The increase becomes very rapid below about 35 K and shows a divergence around 24 K (23.8 K) as shown in Fig. 5 due to the critical slowing down toward a long-range ordered state. Thus, the  ${}^7\text{Li}$  NMR data confirm  $T_N=23.8$  K for this material and provide further evidence for the importance of short-range spin correlations at temperatures well above  $T_N$ , a feature expected for a frustrated spin system.

## B. $\text{Ba}_2\text{YRuO}_6$

### 1. Structural details—Y/Ru order disorder

In the phase diagram of Anderson *et al.*,<sup>2</sup> this compound, with a  $B$ -site formal charge difference of two and size difference of  $\Delta r=0.34$  Å,<sup>13</sup> lies near the border for  $B$ -site order. It is of great interest to determine the degree of  $\text{Y}^{3+}/\text{Ru}^{5+}$  site order which has not been addressed previously. While the

crystal structure of this material, refined from neutron powder-diffraction data, had been reported earlier,<sup>6</sup> a new study was carried out, along with MAS  ${}^{89}\text{Y}$  NMR to address this question. The neutron-scattering lengths for Y and Ru are relatively similar, 7.75 and 7.03 fm, respectively, about a 10% difference. The situation is similar for x-rays with about the same level of contrast, which is somewhat problematic for analysis of powder data for either case. However, in addition to the scattering power at the  $B$  and  $B'$  sites, the  $\text{O}^{2-}$  positional parameter,  $(x\ 0\ 0)$ , is a critical measure of order/disorder. For the fully disordered model, which would be described in  $Pm3m$  rather than  $Fm3m$  with a unit-cell edge of half the length,  $x=\frac{1}{4}$  (retaining the  $Fm3m$  setting) and the  $B$ -O and  $B'$ -O bond lengths would be equal. Thus, the deviation from  $x=\frac{1}{4}$  is a measure of site ordering. As neutrons are more sensitive to oxygen than x rays, this is the diffraction method of choice.

Before proceeding to the results, it is important to review the general situation with  $B$ -site order in double perovskites. While the aforementioned phase diagram of Anderson *et al.* gives a rough guide to the likelihood of  $B/B'$ -site order, more detailed studies exist, especially by Woodward *et al.*<sup>14,15</sup> who have focused on the  $B^{3+}/B^{5+}$  case which is most relevant here. To summarize some of their findings, for  $\Delta r < 0.260$  Å, 100%  $B/B'$ -site order is never found, with one exception. The extent of  $B/B'$ -site order is determined quantitatively by refinement of neutron powder-diffraction data and it is remarked that in all cases of partial order, the  $hkl$  all-odd supercell reflections are measurably broader than the  $hkl$  all-even subcell reflections. For example, among the  $Fm3m$  phases studied,  $\text{Ba}_2\text{YNbO}_6$  is judged to be 100% ordered,  $\Delta r=0.260$  Å while  $\text{Ba}_2\text{ScNbO}_6$  and  $\text{Ba}_2\text{ScTaO}_6$ , with  $\Delta r=0.105$  Å, show only about 50% order. With smaller  $A$ -site ions and lower crystal symmetry, the degree of  $B/B'$ -site order appears to increase for the same combination of ions. For example,  $\text{Sr}_2\text{ScNbO}_6$  and  $\text{Ca}_2\text{ScNbO}_6$ , both  $P2_1/n$  materials, show order levels of 69% and 96%, respectively.  $\text{Ca}_2\text{YNbO}_6$  is classified as 100% ordered. Applying these findings to the specific case of  $\text{Ba}_2\text{YRuO}_6$ , where  $\Delta r$

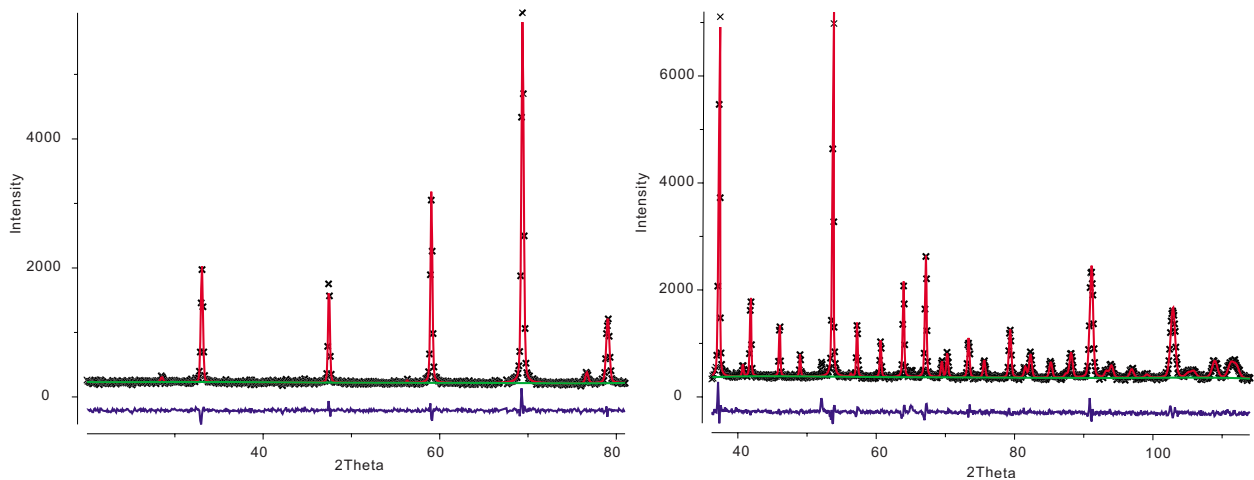


FIG. 6. (Color online) Refinement of the neutron-diffraction data of  $\text{Ba}_2\text{YRuO}_6$  at 297.5 K using the GSAS software package (Ref. 10) for two wavelengths, 2.37 Å, left panel and 1.33 Å, right panel, showing the experimental data (+) and the fit as a solid line. The vertical tick marks represent the Bragg-peak positions and the bottom line is the difference between the calculated and experimental profiles.

TABLE I. The atomic coordinates, isotropic displacement factors at 297.5 K for  $\text{Ba}_2\text{YRuO}_6$  (space group  $Fm\bar{3}m$ ).  $R_{\text{wp}}=0.0571$ ,  $\chi^2=1.6$ , and cell constant  $a=8.33559(9)$  Å. Anisotropic displacements refined for O:  $U_{11}=0.0032(10)$  and  $U_{22}=U_{33}=0.0106(4)$  (Å<sup>2</sup>).

Atom	$x$	$y$	$z$	$U_{\text{iso}}$ (Å <sup>2</sup> )
Ba	0.25	0.25	0.25	0.0067(5)
Y	0.5	0.5	0.5	0.0082(18)
Ru	0	0	0	0.0049(19)
O	0.26513(24)	0	0	0.0103(4)

$=0.34$  Å, one would then expect  $\sim 100\%$   $B/B'$ -site order.

The results of the refinement of the neutron-diffraction data at 299.6 K on a fully ordered  $B/B'$ -site model are shown in Fig. 6 and Tables I and II. The atomic positions and derived interatomic distances are in excellent agreement with those of Ref. 6. The observed atomic displacement parameters,  $U_{\text{iso}}$ , do not suggest that  $B/B'$ -site disorder is significant. The anisotropic  $U_{ij}$  values for the O site are very similar to those obtained for  $\text{Ba}_2\text{YNbO}_6$ , i.e.,  $U_{11} < U_{22}=U_{33}$ , with a somewhat disklike ellipsoid for the site.<sup>14</sup> Attempts to refine the occupation rates of the Y and Ru sites using the constraints applied in Ref. 14 did not yield reasonable values. Refinements imposing a few percent Y/Ru site mixing did yield reasonable results but for mixing greater than  $\sim 5\%$ ,  $U_{\text{iso}}$  for the Ru site became negative. Finally, a comparison of the peak widths of the supercell and subcell reflections, Table III, does not constitute evidence for site disorder, either from the x-ray or neutron data. Taken together, the above observations suggest either negligible or at most, very slight, Y/Ru site mixing.

Nonetheless, the <sup>89</sup>Y MAS NMR data of Fig. 7 present evidence of a low level of site mixing. Here two distinct peaks are seen at chemical shifts of  $-5100$  and  $-5860$  ppm, with integrated areas in the ratio of roughly 7 and  $93 \pm 3\%$ , respectively. Assignment of these peaks and the interpretation of their relative intensities follow the related work of Grey *et al.*<sup>16</sup> where multiple <sup>89</sup>Y MAS NMR peaks observed in pyrochlore oxides  $\text{Y}_{2-x}\text{Ln}_x\text{Ti}_2\text{O}_7$  were interpreted in terms of the number of next-nearest-neighbor cations. In  $\text{Y}_{1.9}\text{Eu}_{.1}\text{Ti}_2\text{O}_7$  for example, peaks were assigned to  $\text{Y}-(\text{O}-\text{Y})_6$  and  $\text{Y}-(\text{O}-\text{Y})_5(\text{O}-\text{Eu})$  with a ratio of intensities of  $\sim 3/1$ . While the Eu substitution level is only 5%, its influence is multiplied by the coordination number at the Y site, six, so the relative intensity of the two NMR peaks is in the ratio 3/1 rather than 20/1. Thus, in the spectrum of  $\text{Ba}_2\text{YRuO}_6$  it is

TABLE II. Interatomic distances between oxygen and the  $B$  ( $B'$ ) site ions.

	Distance (Å)	O-B-O angle (deg)
Y-O	2.2175(20)	90,180
Ru-O	1.9505(20)	90,180

TABLE III. Comparison of peak widths for supercell (all-odd) and subcell (all-even) reflections for  $\text{Ba}_2\text{YRuO}_6$ , both powder neutron and x-ray data.

Reflection	Width (full width at half maximum)	
	(deg)	Ratio (super/sub)
Neutron data 3.8 K		
(111)	0.24(6)	0.98(24)
(200)	0.244(3)	
(331)	0.33(1)	0.90(4)
(420)	0.365(4)	
X-ray data 298 K		
(111)	0.087(4)	1.07(9)
(200)	0.081(3)	

reasonable to assign the major peak at  $-5860$  ppm to the environment  $\text{Y}-(\text{O}-\text{Ru})_6$  and the minor peak at  $-5100$  ppm to  $\text{Y}-(\text{O}-\text{Ru})_5(\text{O}-\text{Y})$ . From the observed relative intensities we infer a Y/Ru mixing level of about 1%. This is certainly consistent with the neutron-diffraction results for  $\text{Ba}_2\text{YRuO}_6$  and illustrates in addition the power of the MAS method in detecting low levels of site mixing. It is worth noting that the <sup>89</sup>Y NMR peaks seen here are shifted significantly out of the known <sup>89</sup>Y chemical shielding range of 60–340 ppm for oxides, even exceeding that of the highly shielded cuprate  $\text{Y}_2\text{BaCuO}_5$  at  $-1250$  ppm,<sup>17</sup> and indicating that a significant amount of unpaired electron density is present at the Y nucleus. A detailed understanding of a shift of this magnitude requires further study.

## 2. Magnetic properties

The magnetic susceptibility for this compound is shown in Fig. 8 and (inset) displays two broad peaks, around 37 and 47 K. The ZFC/FC curves show a slight divergence around 115 K. The inverse magnetic susceptibility was fitted with the Curie-Weiss law giving  $\theta=-571(3)$  K and  $C=2.69(1)$  mol/emu K. The Curie constant is larger than the

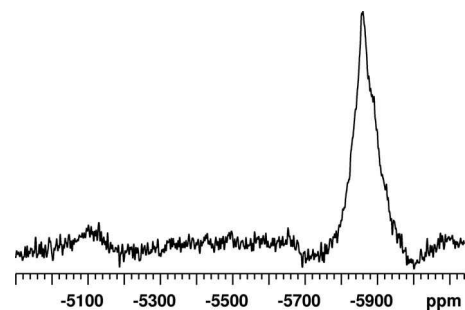


FIG. 7. The <sup>89</sup>Y MAS NMR resonance peaks for  $\text{Ba}_2\text{YRuO}_6$  at room temperature showing two distinct peaks at  $-5100$  and  $-5880$  ppm.

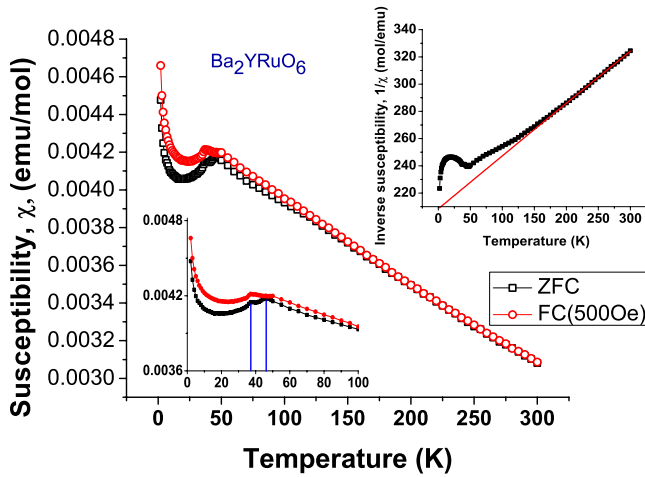


FIG. 8. (Color online) The temperature dependence of the magnetic susceptibility of  $\text{Ba}_2\text{YRuO}_6$ . The insets show clearly the two maxima at 47 and 36 K and the Curie-Weiss behavior.

spin-only value of 1.88 mol/emu K but agrees very well with that reported previously.<sup>6</sup> It is possible that a true Curie-Weiss regime does not exist for this compound below 300 K. The weak upturn in the susceptibility at low temperatures is attributed to paramagnetic impurities. The data below 10 K were fitted to a Curie-Weiss law with an added temperature-independent term with the resulting parameters  $C = 0.001$  mol/emu K,  $\theta = -1.3$  K, and  $\chi(\text{TIP}) = 4.0 \times 10^{-3}$  emu/mol. This indicates that the paramagnetic impurity level is well below 1%.

The observation of two susceptibility maxima was not reported previously<sup>6</sup> and it is unclear which, if either, represents a transition to long-range order. Thus, the heat capacity was measured, as shown in Fig. 9. A sharp  $\lambda$ -type anomaly is evident at 36 K while no feature is observed at 47 K. Therefore, the real transition temperature for  $\text{Ba}_2\text{YRuO}_6$  is 36 K.

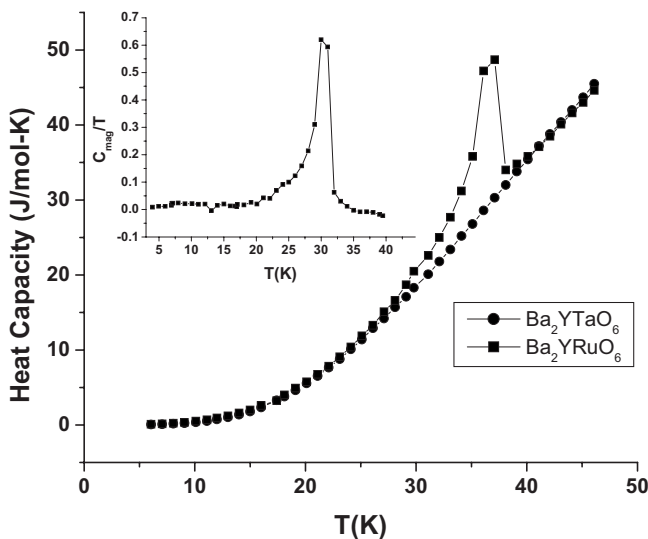


FIG. 9. The heat capacity of  $\text{Ba}_2\text{YRuO}_6$  and its lattice match analog,  $\text{Ba}_2\text{YTaO}_6$ . Note the sharp lambda anomaly at 36 K. The inset shows a plot of  $C_{\text{mag}}/T$  vs  $T$  from which the entropy removal ( $\sim 24\%$  of the theoretical value) was estimated.

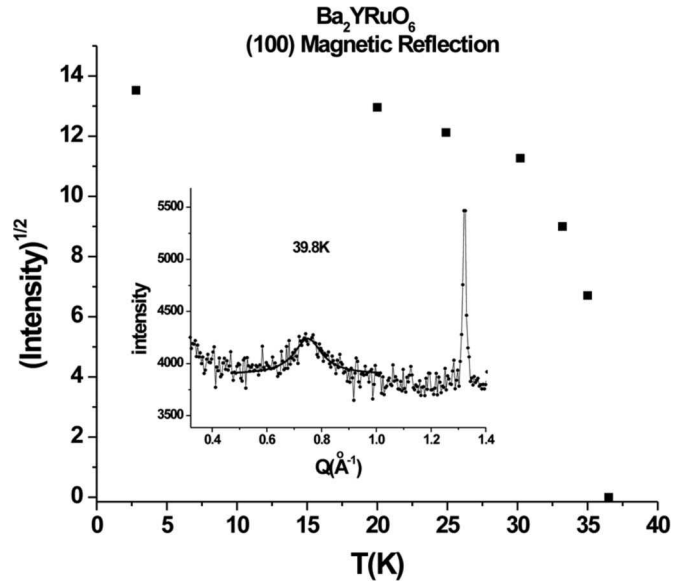


FIG. 10. The intensity of the (100) magnetic reflection versus temperature below 37 K. The data above 30 K have been fitted to extract the critical exponent  $\beta = 0.296(5)$ . The inset shows the broad peak indicative of short-range magnetic correlations at 39.8 K. This feature at  $Q = 0.750(4) \text{ \AA}^{-1}$  is fitted to the standard Ornstein-Zernike Lorentzian line shape (Ref. 16) giving a correlation length,  $\xi = 17(4) \text{ \AA}$ .

This gives a frustration index,  $f \sim 16$  which is slightly smaller than the value of 18 reported earlier but still indicative of a highly frustrated system. The broad susceptibility maximum at  $\sim 47$  K is thus attributed to short-range spin correlations which are expected for a highly frustrated magnet above the critical temperature. The entropy loss below 44 K was estimated for this material from the data shown in the inset of Fig. 9 to be 2.69 J/mol K which is only 24% of the expected value for  $S = \frac{3}{2}$ . This is further evidence for the importance of the postulated short-range correlations above  $T_N$ .

To corroborate the heat-capacity result and add more insight to the interpretation of the susceptibility data, neutron-diffraction measurements were carried out at various temperatures above and below  $T_N$ . The type I fcc magnetic structure reported previously was confirmed with an ordered  $\text{Ru}^{5+}$  moment of  $2.1(1)\mu_B$ , much below the spin-only value of  $3\mu_B$  but again in line with.<sup>6</sup> As well, the temperature dependence of the (100) magnetic reflection, Fig. 10, is consistent with  $T_N = 36$  K. The critical exponent,  $\beta$ , derived from these data is 0.296(5) but the number of data points within the critical region is small and this value cannot be considered as highly accurate. Note also, inset, that magnetic scattering persists in the form of a broad, diffuse feature even at 39.8 K, which is direct evidence for short-range magnetic correlations. This peak was fitted to the standard Ornstein-Zernike Lorentzian of the form  $I(Q) = A / [(Q - Q_0)^2 + \kappa^2]$ , where  $Q = 4\pi \sin \theta / \lambda$  and  $\kappa$  is the inverse correlation length.<sup>18</sup> The derived values are  $Q_0 = 0.750(4) \text{ \AA}^{-1}$  and  $\kappa = 0.06(1) \text{ \AA}^{-1}$ , giving a correlation length,  $\xi = 17(4) \text{ \AA}$ , which is approximately two unit-cell lengths. The origin of this short-range order likely results from the high level of geometric magnetic frustration. Note that the low,  $\sim 1\%$ ,

level of site disorder is insufficient to destroy long-range AF order which is clearly the ground state for this  $S=\frac{3}{2}$  material.

#### IV. SUMMARY AND CONCLUSIONS

Two *B*-site ordered double perovskites,  $\text{La}_2\text{LiRuO}_6$  and  $\text{Ba}_2\text{YRuO}_6$ , with  $\text{Ru}^{5+}$  ( $S=\frac{3}{2}$ ) as the only magnetic ion, have been reinvestigated from the perspective of the geometric magnetic frustration expected for the fcc magnetic lattice. Both are indeed highly frustrated magnets with frustration indices,  $f\sim 9$  and 16 for  $\text{La}_2\text{LiRuO}_6$  and  $\text{Ba}_2\text{YRuO}_6$ , respectively. Heat capacity and  $^7\text{Li}$  NMR data establish  $T_N=23.8$  K in spite of the susceptibility maximum at  $\sim 30$  K for  $\text{La}_2\text{LiRuO}_6$ . The NMR results also show evidence for short-range spin correlations well above  $T_N$ . Evidence for Y/Ru site disorder at the level of about than 1% is found from  $^{89}\text{Y}$  MAS NMR for  $\text{Ba}_2\text{YRuO}_6$ . This latter phase shows a more complex bulk magnetic behavior than reported previously with two maxima at 47 and 36 K. Heat capacity and

neutron-diffraction data establish  $T_N=36$  K. Significant short-range spin correlations are evident above  $T_N$  at 39.8 K with a correlation length of  $\sim 17$  Å which is about two cubic cell edge lengths. In spite of the high levels of frustration in both compounds and the presence of slight Y/Ru site disorder in one, the ground state is long-range AF order for these  $S=\frac{3}{2}$  magnets. Subsequent studies will focus on isostructural  $S=1$  and  $S=\frac{1}{2}$  double perovskites to investigate the role of  $S$  among other factors on the determination of the ground state.

#### ACKNOWLEDGMENTS

We would like to thank to Paul Dube for assistance in measuring susceptibilities and heat capacities at McMaster. J.E.G. and T.I. thank NSERC for Discovery Grants. T.I. also thanks the Canadian Foundation for Innovation and the Canadian Institute for Advanced Research. C.R.W. thanks the NSF for funding through Grant No. DMR-08-04173. S.K. acknowledges CFI and NSERC for support. V. K. M. is grateful to NSERC.

- 
- <sup>1</sup>A. P. Ramirez, *Annu. Rev. Mater. Sci.* **24**, 453 (1994), J. E. Greedan, *J. Mater. Chem.* **11**, 37 (2001).  
<sup>2</sup>M. T. Anderson, K. B. Greenwood, G. A. Taylor, and K. R. Poppelmeier, *Prog. Solid State Chem.* **22**, 197 (1993).  
<sup>3</sup>C. J. Howard and H. T. Stokes, *Acta Crystallogr.* **A61**, 93 (2005).  
<sup>4</sup>C. R. Wiebe, J. E. Greedan, G. M. Luke, and J. S. Gardner, *Phys. Rev. B* **65**, 144413 (2002).  
<sup>5</sup>C. R. Wiebe, J. E. Greedan, P. P. Kyriakou, G. M. Luke, J. S. Gardner, A. Fukaya, I. M. Gat-Malureanu, P. L. Russo, A. T. Savici, and Y. J. Uemura, *Phys. Rev. B* **68**, 134410 (2003).  
<sup>6</sup>P. D. Battle and C. W. Jones, *J. Solid State Chem.* **78**, 108 (1989).  
<sup>7</sup>P. Schiffer and A. P. Ramirez, *Comments Condens. Matter Phys.* **18**, 21 (1996).  
<sup>8</sup>P. D. Battle, C. P. Grey, M. Hervieu, C. Martin, C. A. Moore, and Y. Paik, *J. Solid State Chem.* **175**, 20 (2003).  
<sup>9</sup>J. Rodríguez-Carvajal, *Physica B* **192**, 55 (1993).  
<sup>10</sup>B. H. Toby, *J. Appl. Crystallogr.* **34**, 210 (2001); A. C. Larson and R. B. Von Dreele, Los Alamos National Laboratory Report No. LAUR 86-748, 2004 (unpublished).  
<sup>11</sup>M. E. Fisher, *Philos. Mag.* **7**, 1731 (1962).  
<sup>12</sup>K. Hayashi, G. Demazeau, M. Pouchard, and P. Hagenmuller, *Mater. Res. Bull.* **15**, 461 (1980); J. Darriet, G. Demazeau, and M. Pouchard, *ibid.* **16**, 1013 (1981).  
<sup>13</sup>R. D. Shannon, *Acta Crystallogr.* **A32**, 751 (1976).  
<sup>14</sup>P. Woodward, R.-D. Hoffman, and A. W. Sleight, *J. Mater. Res.* **9**, 2118 (1994).  
<sup>15</sup>P. W. Barnes, M. W. Lufaso, and P. M. Woodward, *Acta Crystallogr.* **B62**, 384 (2006).  
<sup>16</sup>C. P. Grey, M. E. Smith, A. K. Cheetham, C. M. Dobson, and R. Dupree, *J. Am. Chem. Soc.* **112**, 4670 (1990).  
<sup>17</sup>K. J. D. MacKenzie and M. E. Smith, *Multinuclear Solid-State NMR of Inorganic Materials* (Pergamon, New York, 2002).  
<sup>18</sup>Malcom F. Collins, *Magnetic Critical Scattering* (Oxford University Press, New York, 1989).